Volume: 1 Issue: 16 Pages: 96-103

International Journal of Research in Academic World

E-ISSN: 2583-1615
Impact Factor: 4.714

Received: 19/November/2022 Int. J Res. Acad. World. 2022; 1(16):96-103 Accepted: 21/December/2022

Cloud Point Extraction of Remazol Turquoise Blue G-133 Dye Using Non-Ionic Surfactant

[*1]Duraimurugan Alias Saravanan, [2]Mohamedsani Abdulkadir Aba Gissaa, [3]J Saravanan and [4]Muktar Abdu Kalifa

[*1, 2, 4]Department of Chemical Engineering, Mettu University, Ethiopia.

[3]Department of Chemical Engineering, Mohamed Sathak Engineering College, Coimbatore, Tamil Nadu, India.

Abstract

In the present study, the removal of color from wastewater containing Remazol Turquoise Blue G-133 dye (copper phthalocyanine reactive dye) by surfactant mediated cloud point extraction (CPE) in batch mode using Triton X-114 (TX-114) as non-ionic surfactant is discussed. Cloud point extraction is a micelle mediated separation process based on clouding phenomena of non-ionic surfactant. The solute concentrations 25 ppm, 50 ppm, and 75 ppm, and surfactant concentration of about 0.01 M to 0.1 M were used. The physical properties such as density, refractive index, viscosity of surfactant rich and surfactant dilute phases were measured. The operating temperatures are selected based on the cloud point temperature and the performance of the cloud point extraction is analyzed using the phase volume ratio, preconcentration factor, distribution coefficient, and extraction efficiency at different temperatures. The feasibility of the CPE process is also studied using the thermodynamic parameters. The negative value of ΔG^0 signifies the spontaneous phenomena of dye solubilization process. The positive values of $\Delta H0$ points out the endothermic nature dye solubilization process, and the positive values of ΔS^0 indicates that the dye molecules are structured in a more random fashion on the mantle of aqueous hydrophilic chains.

Keywords: Remazol turquoise blue G-133, triton X-114, cloud point temperature, cloud point extraction

1. Introduction

Man-made dyes and pigments are added to the environment by textile, leather, paper, plastic, and printing industries. These industries discharge colored effluents possessing complex chemical structures and retain 5-10% of dye stuffs [1]. The colored compounds tend to persist in the environment, decline the water quality and results in allergies, skin irritation, cancer and mutation [2]. The colored compounds obstruct the absorption of solar rays and alter the photosynthetic activity causing severe decline in the aquatic biodiversity [3]. Reactive dyes are produced in a large scale than any other class of dyes and are favored by the consumer for their bright colors and high wetfastness [4]. Reactive dye belongs to the class copper phthalocyanine with a reactive group of sulfatoethyl sulfone. Copper phthalocyanine dyes are widely used in textile industry and resist the bacterial degradation [3]. Remazol Turquoise Blue-G 133 (RTB G-133) is one such reactive dye based on copper phthalocyanine and is highly preferred owing to its chemical stability, brilliant blue color and high tinctorial strength. The RTB G-133 comprises tetrasulfonated copper phthalocyanine with one to two of the sulfonate groups transformed to linker arms [5]. Reactive dyes are also the most problematic compounds in textile industries wastewater owing to is high solubility in water and needs treatment before disposal to improve the quality of water [6]. Different techniques are available for the removal of color from wastewater including nanofiltration [7] and adsorption onto different substances such as agricultural solid waste [8], micellar-enhanced ultrafiltration [9], different bentonites [10], ozonations [11], several oxidation processes [12,13] various types of activated carbon [14], and surfactant impregnated montmorillonite [15], etc. However, each method has its own limitations. The ultrafiltration and nanofiltration can be used for complete removal of all types of dye, but it is imperative to avoid membrane fouling as it decreases the flux. Due to low biodegradability of dyes, colored effluents cannot be removed efficiently by a conventional biological wastewater treatment process [16]. In the adsorption process, the adsorption capacity is highly affected by the pH of solutions depending on the type of adsorbent and adsorbate.

In the last decade, the potential of aqueous micellar solution in the field of separation science is clearly identified [17]. A novel technology for effluent treatment involves surfactant based separation methods. Cloud point extraction (CPE) is one such method used for removing dye from aqueous solutions. At certain temperature, aqueous solution of a non-ionic surfactant becomes turbid. The further increase in temperature separates the solution in two different phases: surfactant rich phase (also known as coacervate phase) and bulk aqueous solution containing surfactant concentration slightly above the critical micelle concentration (CMC) [18, 19]. A number of authors have investigated the mechanisms for phase separation of non-ionic surfactants above cloud point. The phase separation occurs due to the dehydration of exterior layer of micelles of non-ionic surfactant, intermicellar attractive force, and increase in micellar size [20].

The solubilization of dye occurs in the mantle and the core of the micelles, based on its polarity. The non-polar solubilizates and polar solubilizates are solubilized in the core of micelles and in the mantle, owing to the increase in the aggregation of

***Corresponding Author:** Duraimurugan Alias Saravanan

micelles and the dehydration of the polyoxyethylene chains respectively [19, 21-26]. The physical properties of heterogeneous phases of aqueous micellar solution provide information about the molecular interactions in the mixture. The density, viscosity, and refractive index are essential to understand the thermodynamic behavior of solute or solvent in liquid mixtures [27].

In the present work, CPE of RTB G-133 dye from wastewater using Triton X-114 (TX-114) as non-ionic surfactant is studied. The CPE were carried out for different sets of TX-114 and RTB G-133 concentrations. The physical properties such as density, viscosity, refractive index, and excess molar volumes for the surfactant dilute phase and the surfactant rich phase were determined at 313.15K, 323.15K, and 333.15 K. The effect of various design parameters such as surfactant concentration, dye concentration, and cloud point temperature on the phase-volume ratio, preconcentration factor, distribution coefficient, and extraction efficiency were investigated at different temperatures. The thermodynamic parameters such as change in enthalpy (ΔH^0), change in entropy (ΔS^0) and Gibbs-free energy (ΔG^0) are determined at different temperatures and the feasibility of cloud point extraction with TX-114 for the removal of dyes from aqueous solution is confirmed.

2. Experimental

Material Remazol Turquoise Blue-G 133 (RTB G-133) dye (FW: 576.10, λmax: 624nm, dye content: 97%), and Triton X-114 (t-Octylphenoxy polyoxyethylene ether), with approximately 8-9 ethoxy units per molecule (density at 298.15 K is 1.058 g. ml^{-1}, Mol. Wt.: 537, λmax: 223 nm), was purchased from Sigma-Aldrich, India. The critical micellar concentration (CMC) of TX-114 is 2.1×10^{-4} M at 298.15 K and the cloud point temperature is 296.15 K. RTB G-133 was used as solute; Triton X-114 was used as the non-ionic surfactant.

JASCO UV-Visible spectrophotometer was used for calibration and measuring the dye concentration in dilute phase after phase separation. The densities of surfactant dilute phase and surfactant rich phase were determined using specific gravity bottle (5 ml) and a weighing balance ((Sartorius, Germany) with a precision of ±0.1 mg. The uncertainty of the measured density was ±0.0001. BROOKFIELD (DV-II + PRO) Viscometer is used to measure the viscosity of the solutions. The uncertainty in the viscosity measurements was found to be ±1.0%. The refractive index of surfactant dilute and surfactant rich phases were measured using Abbe Refractometer (Guru Nanak Instruments, New Delhi).refractive index was precise to ±0.0005. Water bath (TECHNICO Laboratory Products, Chennai), was used to maintain the desired temperature for cloud point extraction. The temperatures were maintained with an accuracy of ±273.35 K.

Solution Preparation

An aqueous micellar solution of 50ml was prepared with different concentrations of solute and surfactant. Different concentrations of dye solutions were prepared from stock solution with appropriate dilution. The calibration of UV spectrophotometer was done using the prepared dye solutions. The solute concentrations were varied from 10 ppm to 100 ppm respectively, surfactant concentration were 0.01 M to 0.1M. Solutions were heated above cloud point temperature (CPT) till phase separation was obtained. The concentrations of solute were 25 ppm, 50 ppm, and 75 ppm, while the surfactant concentration was varied from 0.01 M to 0.1 M, respectively. The dye concentrations were kept minimal as 25 ppm, 50 ppm, and 75 ppm, inorder to evaluate the dye removal efficiency [6].

Determination of Cloud Point Temperature

The cloud point of aqueous non-ionic surfactant solution was determined by heating 50 ml of such micellar solution in a conical bottom graduated testtubes using thermostatic water bath. Inorder to determine the cloud point, the temperature was increased at a rate of 274.35 K per min. The temperature at which the micellar solution becomes turbid is visually observed and is referred to as a cloud point temperature. The turbidity appears due to the scattering of visible light by the large surfactant aggregates known as micelles. On heating the turbid solution above the CPT, the solution gets separated into two different phases (surfactant rich phase and surfactant dilute phase). The surfactant rich phase is enriched in surfactant aggregates (micelles), whereas the surfactant dilute phase is depleted of such surfactant micelles. This process is reversible and these heterogeneous mixtures become homogeneous when cooled below the CPT. All the CPT reported were the average of triplicate measurements with an accuracy of ±273.35 K. The experiments were performed for different combinations of surfactant and solute concentrations. The CPT were found to vary in the range of 313.15 K to 333.15 K. Based on these measurements, the operating temperatures were selected.

Cloud Point Extraction of RTB G-133 dye

A 50ml of aqueous micellar solution containing dye and Triton X-114 were prepared with varying concentrations of dye and Triton X-114 in graduated testtubes. The CPE was carried out for different concentrations of dye (i.e., 25 ppm, 50 ppm and 75 ppm), and surfactant (i.e., 0.01M – 0.1M). Each set of samples were kept in the thermostatic bath maintained at desired temperature for 30 min. All the experiments were conducted at temperatures of 313.15 K, 323.15 K and 333.15 K based on the CPT. After the formation of heterogeneous clear phases, the volumes of surfactant-rich phase and dilute phase are noted down. Then the concentration of RTB G-133 dye in dilute phase determined by UV-Visible spectrophotometer. The dye concentration of surfactant dilute phase is analyzed and the surfactant rich phase concentration was obtained using material balance. The physical properties of two phases such as density and refractive index of each phase were measured for the surfactant dilute and rich phases. The phase volume ratio, preconcentration factor, distribution coefficient and extraction efficiency were analyzed. The thermodynamic properties such as change in enthalpy (ΔH^0), entropy (ΔS^0) and Gibb's free energy (ΔG^0) were also evaluated.

Parameters Involved in Cloud Point Extraction

In cloud point extraction, the parameters such as the phase volume ratio (RV), the preconcentration factor (fC), distribution coefficient (Kd) were studied to determine the feasibility of extraction process.

The phase volume ratio (RV) is defined as the ratio of the volume of the surfactant-rich phase to that of the aqueous phase (Eq. (1)). The preconcentration factor (fC) is defined as the ratio of the volume of bulk solution before phase separations (Vt) to that of the surfactant-rich phase after phase separation (Vs) (Eq. (2)). The distribution coefficient (Kd) is defined as the ratio of the concentration of solute in

surfactant-rich phase (Cs) to that of the concentration of solute in dilute phase (Cw) (Eq. (3)).The recovery or extraction efficiency of solute can be calculated as the percentage of solute extracted from the bulk solution into the surfactant-rich phase. It is calculated using the following expression (Eq. (4)).

$$R_V = \frac{V_s}{V_w} \quad (1)$$

$$f_c = \frac{V_t}{V_s} \quad (2)$$

$$K_d = \frac{C_s}{C_w} \quad (3)$$

$$\eta = \frac{(C_0 V_t - C_w) - (V_t - V_s)}{C_0 V_t} X\ 100 \quad (4)$$

Where Vs and Vw are the volumes of the surfactant-rich phase and the aqueous phase, respectively. Vt is the volumes of the bulk solution before phase separation. Cs and Cw are the concentrations of solute in the surfactant-rich phase and the dilute phase, respectively. C0 is the initial concentration of solute in the bulk solution. Vt is the volume of solution.

3. Results and Discussion

In Cloud Point Extraction, the phenomenon of formation of two incompatible phases above CPT is used for the solubilization of the dyes. The phase separation begins as a consequence of either miscibility of micelles or the separation of micelles from water. The physical property of the two phases also aids the phase separation. The density difference between the surfactant-rich phase and surfactant dilute phase result in such physical separation of two different phases [28]. The physical properties such as density, refractive index, and viscosity are necessary to be acquainted with the thermodynamic behavior of solute or solvent in liquid mixtures [27].

Physical Properties of Dilute and Surfactant Rich Phases

The effect of surfactant and solute concentration on the density, refractive index, and viscosities of dilute and surfactant rich phase are given in Table 1, Table 2 and Table 3. The surfactant-rich phase consists of surfactant, dye, and water molecules. The number of micelles and the size of the micelles increase with the increase in surfactant concentration [29]. As a result, the surfactant settles into the surfactant-rich phase and the density difference between the two phase's increases. Again with large number of micelles, more dye solute will be solubilized with surfactant micelles in the surfactant-rich phase. Hence, the density increases with surfactant concentration. The increase in temperature results in the increased solubility of the dye. At higher temperature, the water molecules escape from the external layers of the micelle resulting in the decrease of water content making the solution very dense.

The refractive index of dilute phase is found to be almost nearer to that of refractive index of water (i.e., 1.332, see Table 2) at all concentrations of surfactant. This ensures that the dilute phase obtained after the CPE is similar to that of water. The increase in the solute concentration increases the density, decreasing the speed of light through the medium and thereby increases the refractive index of the medium. Hence the refractive index of the surfactant-rich phase increases with the surfactant concentration and the dilute phase is nearly constant to that of water.

The viscosity of Triton X-114 surfactant is relatively high (i.e., 260 cp at 298.15 K), when compared to that of water (i.e., 0.894 cp at 298.15 K). The viscosity of the mixture strongly depends on the presence of water. As the surfactant concentration increases, the surfactant-rich phase becomes more viscous compared to the dilute phase owing to the molecular attraction between identical structures of the molecules. The increase in the temperature results in the increase in the viscosity of surfactant-rich phase due to the removal of water molecules from the external layers of micelles. Whereas, at higher temperature, the dilute phase viscosity decreases with addition of water molecules due to the weak hydrogen bond interaction and reaches a constant value.

Table 1: Physical properties for 25ppm of surfactant dilute phase and surfactant rich phase at 313.15K, 323.15K and 333.15K.

Surfactant Dilute Phase at 313.15K				Surfactant Rich Phase at 313.15K		
TX-114 (M)	**Density (g cm^{-3})**	**Refractive Index**	**Viscosity (mPa s)**	**Density (g cm^{3})**	**Refractive index**	**Viscosity (mPa s)**
0.02	0.998	1.333	0.89	1.017	1.358	NA
0.04	0.995	1.333	0.90	1.017	1.359	NA
0.06	0.995	1.332	0.88	1.017	1.361	136.2
0.08	0.993	1.332	0.88	1.019	1.362	149.6
0.1	0.991	1.331	0.86	1.021	1.363	145.2
Surfactant dilute phase at 323.15K				**Surfactant rich phase at 323.15K**		
TX-114 (M)	**Density (g cm^{-3})**	**Refractive Index**	**Viscosity (mPa s)**	**Density (g cm^{-3})**	**Refractive index**	**Viscosity (mPa s)**
0.02	1.037	1.331	0.87	1.022	1.358	NA
0.04	1.034	1.332	0.88	1.027	1.359	NA
0.06	1.028	1.331	0.87	1.030	1.360	147.1
0.08	1.027	1.331	0.87	1.035	1.362	159.5
0.1	1.025	1.333	0.90	1.038	1.363	171.3
Surfactant dilute phase at 333.15K				**Surfactant rich phase at 333.15K**		
TX-114 (M)	**Density (g cm^{-3})**	**Refractive Index**	**Viscosity (mPa s)**	**Density (g cm^{-3})**	**Refractive index**	**Viscosity (mPa s)**
0.02	1.039	1.332	0.88	1.031	1.356	NA
0.04	1.031	1.331	0.87	1.033	1.360	NA

0.06	1.029	1.332	0.88	1.034	1.362	159.7
0.08	1.024	1.332	0.88	1.035	1.363	173.8
0.1	1.022	1.333	0.89	1.036	1.365	192.1

Table 2: Physical properties for 50ppm of surfactant dilute phase and surfactant rich phase at 313.15K, 323.15K and 333.15K.

Surfactant dilute phase at 313.15K				**Surfactant rich phase at 313.15K**		
TX-114 (M)	**Density (g cm^{-3})**	**Refractive index**	**Viscosity (mPa s)**	**Density (g cm^{3})**	**Refractive index**	**Viscosity (mPa s)**
0.02	0.998	1.333	1.00	1.023	1.362	NA
0.04	0.996	1.333	0.97	1.024	1.630	NA
0.06	0.995	1.333	0.96	1.025	1.364	145.6
0.08	0.994	1.332	0.96	1.026	1.365	174.1
0.1	0.994	1.332	0.96	1.027	1.371	189.9
Surfactant dilute phase at 323.15K				**Surfactant rich phase at 323.15K**		
TX-114 (M)	**Density (g cm^{-3})**	**Refractive index**	**Viscosity (mPa s)**	**Density (g cm^{-3})**	**Refractive index**	**Viscosity (mPa s)**
0.02	1.033	1.332	0.99	1.024	1.364	NA
0.04	1.032	1.332	0.99	1.025	1.364	NA
0.06	1.031	1.332	0.99	1.026	1.365	153.1
0.08	1.030	1.333	0.98	1.031	1.368	179.3
0.1	1.029	1.333	0.97	1.032	1.371	191.7
Surfactant dilute phase at 333.15K				**Surfactant rich phase at 333.15K**		
TX-114 (M)	**Density (g cm^{-3})**	**Refractive index**	**Viscosity (mPa s)**	**Density (g cm^{-3})**	**Refractive index**	**Viscosity (mPa s)**
0.02	1.035	1.332	0.99	1.032	1.362	NA
0.04	1.034	1.332	0.98	1.034	1.361	NA
0.06	1.033	1.332	0.98	1.035	1.366	162.4
0.08	1.032	1.332	0.98	1.036	1.366	183.9
0.1	1.031	1.333	0.98	1.036	1.368	196.5

Table 3: Physical properties for 75ppm of surfactant dilute phase and surfactant rich phase at 313.15K, 323.15K and 333.15K.

Surfactant dilute phase at 313.15K				**Surfactant rich phase at 313.15K**		
TX-114 (M)	**Density (g cm^{-3})**	**Refractive index**	**Viscosity (mPa s)**	**Density (g cm^{3})**	**Refractive index**	**Viscosity (mPa s)**
0.02	0.998	1.331	0.86	1.022	1.361	NA
0.04	0.998	1.332	0.88	1.025	1.361	NA
0.06	0.997	1.332	0.9	1.027	1.362	157.3
0.08	0.996	1.334	0.88	1.028	1.368	179.6
0.1	0.994	1.332	0.9	1.029	1.372	195.8
Surfactant dilute phase at 323.15 K				**Surfactant rich phase at 323.15K**		
TX-114 (M)	**Density (g cm^{-3})**	**Refractive index**	**Viscosity (mPa s)**	**Density (g cm^{-3})**	**Refractive index**	**Viscosity (mPa s)**
0.02	1.034	1.332	1.00	1.025	1.364	NA
0.04	1.033	1.333	0.99	1.028	1.364	NA
0.06	1.032	1.332	0.99	1.030	1.366	160.7
0.08	1.031	1.332	0.98	1.032	1.371	188.4
0.1	1.03	1.332	0.98	1.033	1.371	201.2
Surfactant dilute phase at 333.15 K				**Surfactant rich phase at 333.15K**		
TX-114 (M)	**Density (g cm^{-3})**	**Refractive index**	**Viscosity (mPa s)**	**Density (g cm^{-3})**	**Refractive index**	**Viscosity (mPa s)**
0.02	1.035	1.33	1.00	1.033	1.362	NA
0.04	1.034	1.332	0.99	1.034	1.361	NA
0.06	1.034	1.331	0.99	1.036	1.364	169.5
0.08	1.033	1.331	0.99	1.037	1.365	190.3
0.1	1.032	1.332	0.99	1.038	1.366	208.6

Phase volume ratio

The phase volume ratio increases with increase in surfactant (Triton X-114) concentration and solute (RTB G-133) concentration and is shown in Fig.1. For an instance, Fig.1 also shows that at a constant temperature of 333.15 K and a surfactant concentration of 0.1 M, the phase volume ratio increases from 29.87 to 46.19 for an increase in dye concentration from 25 ppm to 75 ppm. Similarly for a constant temperature of 333.15 K and a lower surfactant concentration of 0.01 M, the phase volume ratio increases from 2.45 to 5.93 for an increase in dye concentration from 25 ppm to 75 ppm. The increase in surfactant concentration

resulted in increase in phase volume ratio owing to the increase in the volume of coacervate phase. So, at higher surfactant concentration, the additional amount of surfactant enters the coacervate phase (surfactant-rich phase) and maintains the material balance as the concentration of surfactant remains constant and near CMC in the dilute phase [15, 21]. However, for a constant dye concentration, the phase volume ratio decreased with the increase in temperature. The effect of operating temperature on the phase volume ratio at a constant dye concentration is shown in Fig.1. As the temperature increases, interaction among micelles of TX-114 will be predominant and dehydration takes place from external layers of micelles. This results in the reduction in the volume of coacervate phase. Hence the phase volume ratio decreases with increase in operating temperature [22].

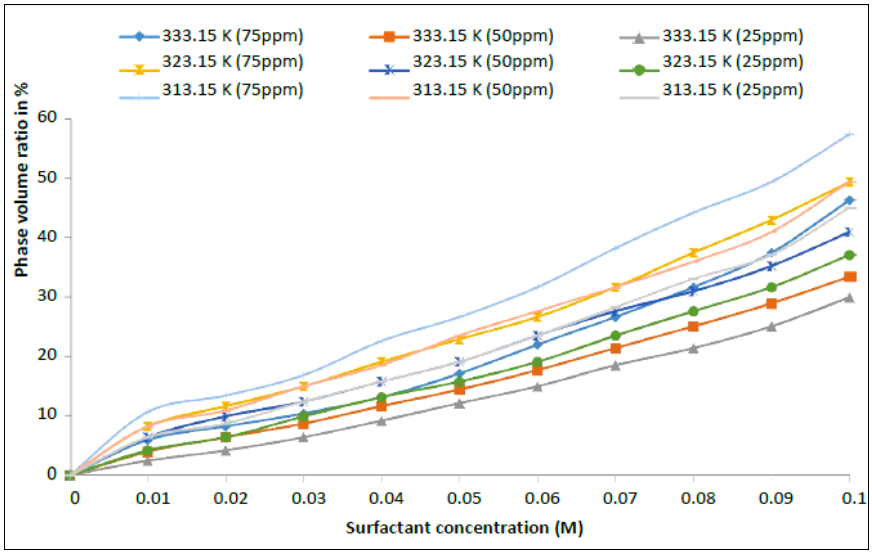

Fig 1: Phase volume ratio versus surfactant concentration for different ppm of dye solution (25 ppm, 50 ppm, and 75 ppm) and different temperatures (313.15 K, 323.15 K and 333.15 K).

Preconcentration Factor

The preconcentration factor decreases with increase in surfactant (Triton X-114) concentration and solute (RTB G-133) concentration and is shown in Fig.2. For example, at a constant temperature of 333.15 K and a surfactant concentration of 0.1 M, the phase volume ratio increases from 29.87 to 46.19 for an increase in dye concentration from 25 ppm to 75 ppm. The preconcentration factor increased with increase in operating temperature, because the surfactant-rich phase volume decreased at higher operating temperature, affecting the high extraction of solute in less surfactant-rich phase volume Fig.2. On the other hand, the preconcentration factor was found to be decreased with increase in both surfactant concentration and solute concentration (Fig.2.). Due to high solubility of the solute in the surfactant micelles, the surfactant-rich phase is low [19], and the solute concentration in the surfactant-rich phase became very high. Therefore, it is because of the higher solubility of solute that the preconcentration factor decreased with increase in surfactant as well as solute concentrations {22-26}.

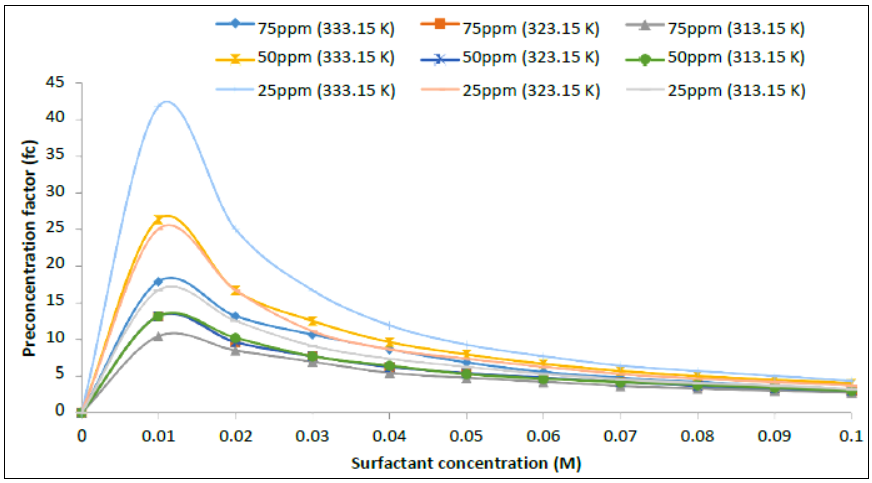

Fig 2: Preconcentration factor versus surfactant concentration for different ppm of dye solution (25 ppm, 50 ppm, and 75 ppm) and different temperatures (313.15 K, 323.15 K and
333.15 K).

Distribution Coefficient

The distribution coefficient increases with the increase in surfactant concentration and decreases with solute concentration and is illustrated in Fig.3. For example, at 333.15 K with a constant solute concentration of 25 ppm, distribution coefficient increases from 5.28 to 65.14 with increase in surfactant concentration from 0.01 M to 0.1 M. It is evident that for a constant feed dye concentration and temperature, the increase in surfactant concentration

solubilized more solutes to the surfactant-rich phase resulting in the concentrated coacervate phase.

The distribution coefficient decreases from 65.14 to 21.63 with increase in solute concentration from25 ppm to 75 ppm for a constant temperature and surfactant concentration of 333.15 K and 0.1 M respectively. The distribution coefficient decreases for a particular surfactant concentration and temperature, owing to the increase in the water content in the surfactant rich phase. In terms of temperature, for a constant solute concentration of 75 ppm and a surfactant concentration of 0.1 M, distribution coefficient increases from 10.81 to 21.63 with rise in temperature from 313.15 K to 333.15 K. At lower temperature, repulsive micellar interaction prevails reducing the micellar aggregation, whereas at higher temperature, attractive micellar interaction is predominant ensuing increased micellar aggregation in the surfactant-rich phase. This results in increased dye solubilization into the surfactant rich phase leading to a higher distribution coefficient.

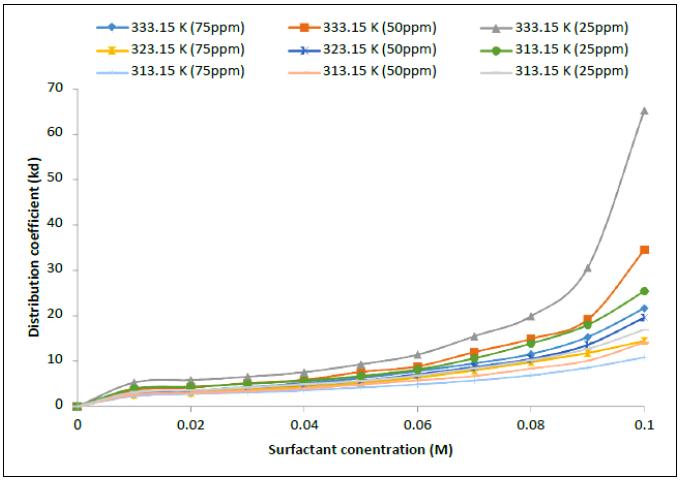

Fig 3: Distribution coefficient versus surfactant concentration for different ppm of dye solution (25 ppm, 50 ppm, and 75 ppm) and different temperatures (313.15 K, 323.15 K and 333.15 K).

Extraction efficiency

At a constant temperature and dye concentration, the extraction efficiency of dye increases with the feed surfactant concentration and is shown is Fig. 4. An extraction efficiency of 98.49% is obtained for 25 ppm solute concentration and at 333.15 K. The concentration of the micelles increases with the increase in feed surfactant concentration, resulting in more solubilization of dyes into the micelles present in the surfactant-rich phase. Consequently, the surfactant concentration in the dilute phase remains around CMC [30]. The extraction efficiency of dye decreases with increase in solute concentration for a particular temperature and surfactant concentration. The added solute remains in the dilute phase at fixed surfactant concentration and operating temperature, decreasing the extraction efficiency of dye. The extraction efficiency increases with increase in temperature. The extraction efficiency of dye increases from 94.40% to 98.49% as the temperature increases from 313.15 K to 333.15 K, for a surfactant concentration of 0.1 M and solute concentration of 25 ppm. The increase in temperature results in increase in aggregation number and more micellar attraction, thereby increasing the solubilization of dye at higher temperatures [21].

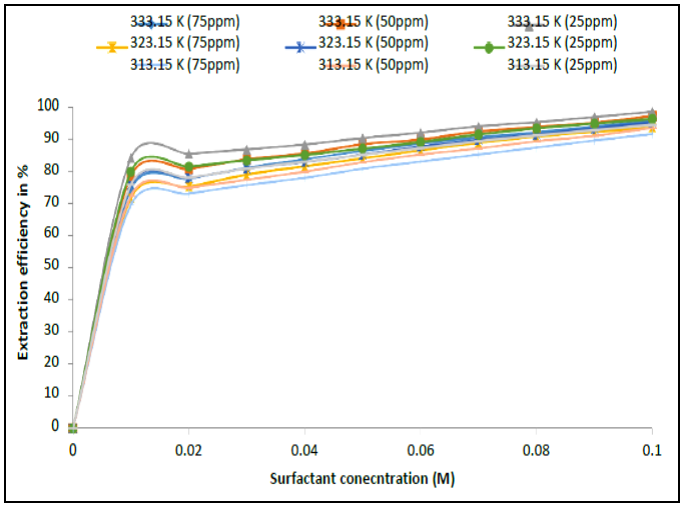

Fig 4: Extraction efficiency versus surfactant concentration for different ppm of dye solution (25 ppm, 50 ppm, and 75 ppm) and different temperatures (313.15 K, 323.15 K and 333.15 K).

Thermodynamic Parameters

Thermodynamic parameters are used to establish the possible mechanism for Cloud Point Extraction of dyes and provide an idea about the feasibility of the process [31]. Different thermodynamic parameters, such as ΔG^0, ΔS^0 and ΔH^0, for the Cloud Point Extraction of Remazol Turquoise Blue G-133 dye were calculated using Eqs. (6) to (10) as follows.

$$\log \frac{q_e}{C_e} = \frac{\Delta S^0}{2.303\ R} + \frac{-\Delta H^0}{2.303RT} \quad (6)$$

$$\Delta G^0 = \Delta H^0 - T\Delta S^0 \quad (7)$$

Where

$$q_e = \frac{Moles\ of\ dye\ solubilized}{Moles\ of\ TX{-}100\ used} = \frac{A}{X} \quad (8)$$

$$A = V_0 C_0 - V_d C_e \quad (9)$$

$$X = C_s V_0 \quad (10)$$

Where T is the temperature in Kelvin. qe/Ce is called the solubilization affinity. qe is the mole of dye solubilized per mole of non-ionic surfactant. *A* is the moles of dye solubilized in the micelles. *V*0 and *V*d are the volume of the feed solution and that of the dilute phase after CPE, respectively. *C*0 and Cs are the concentrations of surfactant in feed. ΔS^0 and ΔH^0can be obtained from a plot of log (qe/Ce) versus (1/T), from Eq. (6). Once these two parameters are obtained, ΔG^0can be determined from Eq. (7).

Change of Enthalpy (ΔH^0) of CPE

The variation in enthalpy change (ΔH^0) during CPE of Remazol Turquoise Blue G-133 dye at different concentrations of TX-114 – RTB G-133 dye are shown in Table 4. It is evident that the value ofΔH^0 increases with TX-114 concentration but decreases with the dye concentration. The positive values of ΔH^0 indicate that the solubilization of dye is endothermic in nature. For an instance, at 25 ppm dye concentration, ΔH^0 value is 22631.92 J/mole for 0.01 M surfactant concentration and increases to 58264.75 J/mole for 0.1 M. The increase in ΔH^0 is due to the increase in the amount of dye solubilization with increase in surfactant concentration.

Then, for a constant 0.1 M surfactant concentration, ΔH^0 decreases from 58264.75 J/mole to 29965.28 J/mole for 25 ppm and 75 ppm respectively. The decrease in ΔH^0 value with increasing dye concentration at a fixed surfactant concentration is due to the decrease in the amount of dye solubilization per mole of surfactant [32, 29].

Change of Entropy (ΔS^0) of CPE

The variations of entropy change (ΔS^0) during CPE of Remazol Turquoise Blue G-133 dye at different concentrations of Triton X-114 – RTB G-133 are shown in Table 4. The entropy changes are positive. It reflects good affinity of the dye molecules towards the surfactant micelles. It is found that the change in entropy (ΔS^0) increases with surfactant concentration but decreases with dye concentration for all the systems. Entropy depends on unsolubilized dye molecules and free surfactant molecules in the CPE system. For an instance, at 25 ppm dye concentration, ΔS^0 value is 92.06 J/mole.K for 0.01 M surfactant concentration and increases to 200.09 J/mole.K for 0.1 M. The increase in ΔS^0 value with surfactant concentration is probably due to the increase of free surfactant molecule in the dilute phase. On the other hand, it has already been reported in dilute phase that CMC of surfactant molecule decreases with increase in dye concentration at a fixed surfactant concentration [31].

Change in Gibbs free energy (ΔG^0) of CPE

The values of Gibbs free energy (ΔG^0) can be calculated from the enthalpy of solubilization (ΔH^0) and the entropy of solubilization (ΔS^0). Table 4 shows the variations of Gibbs free energy change (ΔG^0) with temperature at a constant dye concentration and different surfactant concentrations. The Change in Gibbs free energy (ΔG^0) values is negative for all the experiments. The negative values of ΔG^0 indicate that the dye solubilization is a spontaneous process and thermodynamically favorable On the one hand, ΔG^0 increases linearly with temperature. For a constant dye concentration of 25 ppm and 0.01 M surfactant concentration, the negative value of ΔG^0 is 6182.69 J/mole for 313.15 K and it increases to 8023.88 J/mole for 333.15 K. The increase in negative values of ΔG^0 with temperature implies the greater driving force for the solubilization of dye and is confirmed by the greater extent of dye extraction with increase in temperature [31]. On other hand, ΔG^0 decreases with increase in surfactant and dye concentrations. For a constant dye concentration of 25 ppm and a temperature of 333.15 K, the negative value of ΔG^0 is 8023.88 J/mole for 0.01 M surfactant concentration and it decreases to 5139.02 J/mole for
0.04 M surfactant concentration. Table 4 presents the change of ΔG^0 with initial Remazol Turquoise Blue G-133 concentrations. Table 4 shows that the value of ΔG^0 decreases with dye and surfactant concentrations at constant temperature in the micellar phase, consequently the amount of dye solubilization per mole of surfactant micelle decreases.

Table 4: Table shows the change of ΔG0 with initial Remazol Turquoise Blue G-133 concentrations.

S. No	T (K.)	S	25 ppm			50 ppm			75 ppm		
			ΔS (J/mol K)	ΔH (J/mol)	ΔG (J/mol)	ΔS (J/mol K)	ΔH (J/mol)	ΔG (J/mol)	ΔS (J/mol K)	ΔH (J/mol)	ΔG (J/mol)
1	313	0.01	92.059	22631.92	-6182.69	64.028	14316.32	-5724.46	51.085	10632.41	-5357.06
2	323	0.01	92.059	22631.92	-7103.28	64.028	14316.32	-6364.74	51.085	10632.41	-5867.91
3	333	0.01	92.059	22631.92	-8023.88	64.028	14316.32	-7005.02	51.085	10632.41	-6378.76
4	313	0.02	83.596	21463.95	-4701.73	60.275	14599.7	-4266.44	48.0595	11045.99	-3996.58
5	323	0.02	83.596	21463.95	-5537.7	60.275	14599.7	-4869.19	48.0595	11045.99	-4477.18
6	333	0.02	83.596	21463.95	-6373.66	60.275	14599.7	-5471.95	48.0595	11045.99	-4957.77
7	313	0.03	74.655	19300.32	-4066.6	68.183	17780.04	-3561.23	46.662	11135.98	-3469.1
8	323	0.03	74.655	19300.32	-4813.15	68.183	17780.04	-4243.06	46.662	11135.98	-3935.71
9	333	0.03	74.655	19300.32	-5559.7	68.183	17780.04	-4924.89	46.662	11135.98	-4402.33
10	313	0.04	72.989	19166.29	-3679.24	65.253	17224.77	-3199.56	54.416	13971.67	-3060.59
11	323	0.04	72.989	19166.29	-4409.13	65.253	17224.77	-3852.1	54.416	13971.67	-3604.76
12	333	0.04	72.989	19166.29	-5139.02	65.253	17224.77	-4504.63	54.416	13971.67	-4148.92
13	313	0.05	79.403	21349.06	-3504.14	73.314	19874.73	-3072.68	52.655	13483.42	-2997.49
14	323	0.05	79.403	21349.06	-4298.17	73.314	19874.73	-3805.82	52.655	13483.42	-3524.03
15	333	0.05	79.403	21349.06	-5092.2	73.314	19874.73	-4538.96	52.655	13483.42	-4050.58
16	313	0.06	82.275	22248.98	-3503.18	69.829	18752.71	-3103.96	55.661	14404.39	-3017.42
17	323	0.06	82.275	22248.98	-4325.93	69.829	18752.71	-3802.26	55.661	14404.39	-3574.02
18	333	0.06	82.275	22248.98	-5148.69	69.829	18752.71	-4500.55	55.661	14404.39	-4130.63
19	313	0.07	96.195	26461.35	-3647.76	89.532	24910.43	-3113.1	68.853	18620.6	-2930.43
20	323	0.07	96.195	26461.35	-4609.71	89.532	24910.43	-4008.42	68.853	18620.6	-3618.96
21	333	0.07	96.195	26461.35	-5571.67	89.532	24910.43	-4903.74	68.853	18620.6	-4307.49
22	313	0.08	104.62	28912.18	-3833.87	90.604	25063.61	-3295.53	71.074	19166.29	-3079.93
23	323	0.08	104.62	28912.18	-4880.07	90.604	25063.61	-4201.57	71.074	19166.29	-3790.67
24	333	0.08	104.62	28912.18	-5926.27	90.604	25063.61	-5107.62	71.074	19166.29	-4501.42
25	313	0.09	134.107	37911.34	-4064.02	99.967	27782.5	-3507.24	90.738	25274.23	-3126.86

Conclusion

The CPE of RTB G-133 using TX-114 as non-ionic surfactant was performed. The effect of surfactant and solute concentration for different set of operating temperatures on

CPE was investigated. The effect of surfactant and dye concentration and temperature on the phase volume ratio, preconcentration factor, distribution coefficient and extraction efficiency were determined. Thermodynamic parameters such as change in Gibbs free energy (ΔG^0), change in enthalpy (ΔH^0) and change in entropy (ΔS^0) of CPE of Triton X-114 – Remazol Turquoise Blue dye system were also studied. Thermodynamic studies confirmed that the CPE is feasible and can be integrated in the textile or other dye processing industries for the treatment of colored effluents. All the experiments were done in batch mode. However, for this novel technology to be applied in large scale, experimental evaluation should be performed in continuous mode. Scale up also requires the study of variation of different design parameters in continuous mode.

Acknowledgments
The authors are grateful to the Department of Chemical Engineering, Mettu University Ethiopia.

References

1. Moussavi G, Khosravi R. Chem. Eng. Res. Des. 2011; 89(10):2182-2189.
2. Ray PK. J. Sci. Indust. Res. 1986; 45:370-371.
3. Silva MC, Corrêa AD, Amorim MTSP, Parpot P, Torres JA, Chagas PMB, J. Mol. Catal. B: Enzym. 2012; 77:9-14.
4. Aspland JR. Textile Chemist and Colorist. 1992; 2431-36.
5. Dursun A, Tepe O, Dursun G. Environ. Sci. Pollut. Res. 2013; 20(1):431-442.
6. Vaigan AA, Moghaddam MRA, Hashemi H, Iran. J. Environ. Health. Sci. Eng. 2009; 6(1):11-16.
7. Chakraborty S, Purkait MK, DasGupta S, De S, Basu JK. Sep. Purif. Technol. 2003; 31(2):141-151.
8. Namasivayam C, Kavitha D. Dyes and Pigments. 2002; 54(1)47-58.
9. Purkait MK, DasGupta S, De S. Sep. Purif. Technol. 2004; 37(1):81-92.
10. Arvanitoyannis I, Eleftheriadis I, Tsatsaroni E. Chemosphere. 1989; 18(9-10):1707-1711.
11. Lin SH, Lin CM. Water Research. 1993; 27(12):1743-1748.
12. Lin SH, Lin C.M. Water Research. 1993; 27(12):1743-1748
13. Majcen-Le Marechal A, Slokar YM, Taufer T. Dyes and Pigments. 1997; 33(4):281-298.
14. Neamtu M, Yediler A, Siminiceanu I, Macoveanu M, Kettrup A. Dyes and Pigments. 2004; 60(1):61-68.
15. Kannan N, Sundaram MM. Dyes and Pigments. 2001; 51(1):25-40.
16. Bae JH, Song DI, Jeon YW. Sep. Sci. Technol. 2000; 35(3):353-365.
17. Golder AK, Hridaya N, Samanta AN, Ray S, Hazard J. Mater. 2005; 127(1-3):134-140.
18. Gullickson ND, Scamehorn JF, Harwell JH, Liquid-coacervate extraction Surfactant Based Separation Processes. Marcel Dekker Inc, New York, 1989, 139-152.
19. Imchuwanit WK, Osuwan S, Scamehorn JF, Harwell JH, Haller KJ. Sep. Sci. Technol. 2000; 35(13):1991-2002.
20. Pool R, Bolhuis PG. Phys. Chem. Chem. Phys. 2010; 12(44):14789-14797.
21. Stalikas CD, TrAC. Trends in Analytical Chemistry. 2002; 21(5):343-355.
22. MK Purkait, Vijay SS, DasGupta S, De S. Dyes and Pigments. 2004; 63(2):151-159.
23. Arunagiri A, John I, Ponnusamy K, Anantharaj R. *Engineering Science and Technology, an International Journal*. 2014; 17(3):137-144.
24. Arunagiri A, Kalaichelvi P, Cherukuria S, Vijayana A. *Int. J Chem. Environ. Eng*. 2012; 3(1):16-23.
25. Joarder R, Santra D, Marjit S, Sarkar M, Eur. Chem. Bull. 2014; 3(6):612-616.
26. Purkait MK, Banerjee S, Mewara S, DasGupta S, De S. Water Res. 2005; 39(16):3885-3890.
27. Purkait MK, DasGupta S, De S, Hazard J. Mater. 2006; 137(2):827-835.
28. Arunagiri A, Purushothaman P, Ponnusamy K, Anantharaj R, Thermodyn J. 2014; 28:1-16..
29. Quina FH, Hinze WL, Ind. Eng. Chem. Res. 1999; 38 (11):4150-4168.
30. Carabias-Martínez R, Rodríguez-Gonzalo E, Moreno-Cordero B, Pérez-Pavón JL, García-Pinto C, Fernández Laespada E, Chromatogr J. 2000; 902(1):251-265.
31. Li JL, Chen BH, Colloid J, Interface. Sci. 2003; 263(2):625-632.
32. Purkait MK, DasGupta S, De S. Desalination. 2009; 244(1-3):130-138.
33. Purkait MK, DasGupta S, De S. Sep. Purif. Technol. 2006; 51(2):137-142.